

Cite this: *Chem. Sci.*, 2021, 12, 50

All publication charges for this article have been paid for by the Royal Society of Chemistry

Received 6th July 2020
Accepted 14th November 2020

DOI: 10.1039/d0sc03715j

rsc.li/chemical-science

Supramolecular strategies in artificial photosynthesis

Tom Keijer, Tessel Bouwens, Joeri Hessels and Joost N. H. Reek *

Artificial photosynthesis is a major scientific endeavor aimed at converting solar power into a chemical fuel as a viable approach to sustainable energy production and storage. Photosynthesis requires three fundamental actions performed in order; light harvesting, charge-separation and redox catalysis. These actions span different timescales and require the integration of functional architectures developed in different fields of study. The development of artificial photosynthetic devices is therefore inherently complex and requires an interdisciplinary approach. Supramolecular chemistry has evolved to a mature scientific field in which programmed molecular components form larger functional structures by self-assembly processes. Supramolecular chemistry could provide important tools in preparing, integrating and optimizing artificial photosynthetic devices as it allows precise control over molecular components within such a device. This is illustrated in this perspective by discussing state-of-the-art devices and the current limiting factors – such as recombination and low stability of reactive intermediates – and providing exemplary supramolecular approaches to alleviate some of those problems. Inspiring supramolecular solutions such as those discussed herein will incite expansion of the supramolecular toolbox, which eventually may be needed for the development of applied artificial photosynthesis.

1 Introduction

Humanity has a solar-power debt as we have been using fossil energy, which was collected by photosynthetic organisms over the course of millions of years, in a faster rate than is currently generated, leading to high CO₂ emissions and climate change as a result. Sustainable energy is sufficiently available; one hour of incident solar power is enough to account for the yearly worldwide energy consumption.¹ Decades of research into crystalline silicon solar cells resulted in the production of sustainable electricity on industrial scale for commercially competitive prices. However, 80% of the energy is consumed in the form of fuel, and it is likely that fuels will remain important in the future. Moreover, electrical power is not easily stored and transported.² Combined with the mismatch in energy demand and solar energy supply due to the day/night cycle and the seasonal fluctuations, various energy storage strategies should be developed to allow the transition to a society that runs on sustainable energy.³ In this context, the production of a chemical fuel by converting solar-energy to fuel (a solar-fuel), by direct or indirect means, is crucial. Plants and cyanobacteria have been converting solar energy to fossil fuel for millions of years already.⁴ As such they form an inspiring example, or even a blue print, to generate man-made devices that directly

produce fuels from solar energy, often referred to as artificial photosynthesis.^{2,5–7}

1.1 The fundamental actions of photosynthesis

For both natural and artificial photosynthesis, the same three fundamental actions are required to convert solar energy into a fuel. (i) Light-harvesting, (ii) charge-separation and (iii) redox catalysis (Fig. 1).^{8,9} Nature has evolved to highly dedicated and ordered, but complex supramolecular architectures, that can capture the light, and transmit the energy with high efficiency.



Fig. 1 The fundamental actions of photosynthesis. (1) Light harvesting. (2) Charge-separation. (3) Redox catalysis. Notice that energy transfer occurs between chromophores (green arrows) after excitation to funnel the energy to the special pair where it leads to charge separation. Some energy losses are required to drive the charge separation forward. Charges are moved to catalysts that drive uphill chemical reactions. Adapted with permission from ref. 8.

Homogeneous Supramolecular and Bio-inspired Catalysis, Van't Hoff Institute for Molecular Sciences (HIMS), University of Amsterdam (UvA), Science Park 904, 1098 XH Amsterdam, The Netherlands. E-mail: j.n.h.reek@uva.nl





Fig. 2 Operational mode of the DSSC (top) and schematic diagram of a DS-PEC (bottom). (A) Dyes anchored on a semiconductor deposited on conducting FTO glass are excited by light. (B) The dye performs charge-separation and (C) oxidizes or reduces the redox couple (RC) in the electrolyte that delivers the charge to the counter electrode (CE) closing the circuit. For n-type the dye is excited (process 1) followed by fast electron injection into the conduction band (CB) (process 2). The dark colour represents the dyes in the depicted electron configuration. The dye is oxidatively quenched by the redox couple (RC) (process 3). The RC is then regenerated at the counter electrode (CE) (process 4). In p-type the electrons move the other way around, but the processes are equivalent to n-type. The dye is excited (process 1) after which it is reductively quenched by an electron in the valence band (VB) of the NiO. The electron of the reduced dye is transferred to the RC (process 3) after which the redox mediator is regenerated at the CE. The possible recombination pathways are depicted with red arrows. A DS-PEC performs processes (A) & (B) in a similar fashion. Process (C) is altered by substituting the RC for a redox catalyst performing reactions such as water splitting. The catalyst may be anchored to the semiconductor surface or dye as diffusion is not required. Water oxidation catalysts (WOC) oxidize water to oxygen and protons. Four oxidations are required to generate a single oxygen molecule. The hydrogen evolution catalyst (HEC) combines the electrons and protons liberated at the anode to form hydrogen gas at the cathode. Every hydrogen molecule requires two electrons from the HEC. The half reactions are often separated by a proton exchange membrane (PEM).

regenerated at the counter electrode. Forward electron propagation is depicted in Fig. 2 with green arrows and this pathway leads to photocurrent. The recombination pathways (red arrows), are non-productive pathways responsible for efficiency losses in these devices. These processes are mainly the neutralization of the ionized dye by charges from the semiconductor (Fig. 2, path 6), regeneration of the redox mediator by the semiconductor of the working electrode (Fig. 2, path 7), and the excited electron decaying to the ground state before injection (Fig. 2, path 5). Recombination pathway 7 is readily minimized by passivation of the surface *via* Al₂O₃ deposition for example. Similar processes occur for both n-type and p-type DSSC, but because the charge mobility in NiO is much lower the charge recombination events are more dominant in p-type cells. Attempts to circumvent charge recombination have mainly focused on finetuning the properties of the dyes.^{32–35} So called push-pull dyes prevent charge-recombination, since it leads naturally to an increased distance between the oxidized

(for n-type) part of the dye and the surface, typically, minimizing recombination pathway 5. This has led to huge efficiency gains for n-type up to 14.7%.³⁶ Currently, the p-type electrodes suffer most from recombination, the record for p-type solar cells is 2.51%.³⁷ In order to have a working DS-PEC, analogous n-/p-type electrodes need to be coupled to catalysts that oxidize water at the anode (n-type) and produce fuel at the cathode (p-type). The low efficiencies observed for p-type DSSC will limit p-type electrodes and hence the overall efficiency of the tandem DS-PEC design. Interestingly, supramolecular strategies are emerging as a viable option to inhibit charge recombination in these devices. In this perspective we will highlight supramolecular strategies to reduce charge recombination in DSSC that act as stepping stones to efficient supramolecular artificial photosynthesis using the tandem DS-PEC design.

2.2.4 Design of DS-PEC. In DS-PEC charge equivalents are directly used to drive chemical reactions instead of solely producing current.³⁸ The eventual stand-alone devices that



chromophores. When porphyrins are metallated, coordination of axial ligands is possible. Several strategies employ this axial binding to produce discrete supramolecular assemblies. Zn-porphyrins are well explored, where coordination occurs at only one axial position. These mainly consist of pyridinyl and imidazolyl metal coordination.

Pyridine–Zn interactions show binding constants of 10^3 – 10^4 M in apolar solvents and therefore supramolecular assemblies use multiple interactions to produce more stable structures under dilute conditions. Often the porphyrins have a double function, acting as the structural backbone and light-harvesting functionality. For example, Zn^{II}-porphyrins can be combined with pyridine substituted free base porphyrins. The fluorescence of Zn^{II}-porphyrins overlaps with the Q-band absorption of the free base porphyrins. The excited Zn^{II}-porphyrin molecule transfers energy to the freebase porphyrin. Complex architectures, like supramolecular porphyrin cages, boxes, ladders and rings could be formed this way. All these assemblies show fast (picosecond) energetically downhill energy transfer processes enhanced by supramolecular pre-organization. Supramolecular assemblies have been thoroughly studied for the purpose of PET and CS,⁴⁵ such as self-assembled dimers of porphyrins and fullerenes as well as trimers and porphyrin squares.⁴⁶ Another strategy is to use a rigid pyridine functionalized template to organize porphyrins in close proximity, resulting in rapid energy transfer among the chromophores.⁴⁷ In addition to axial binding, functionalization of porphyrin macrocycles with specific binding motifs can result in supramolecular organization of chromophore arrays using metal–ligand, hydrogen bonding, ion–dipole and π – π stacking interactions.⁴⁸ When these interactions are adequately chosen, extensive arrays (J-aggregates) can be formed *via* self-assembly, which show energy transfer over large distances.⁴⁹ A complementary approach comprises the use of a scaffold such as a polymer or dendrimer, and by means of its functionalities induce supramolecular organization. A plethora of scaffolds has been explored, including (viral) proteins, DNA, and lipid membranes, (non-natural) peptides and dendrimers.⁴³

The supramolecular interactions used to properly pre-organize chromophores, can also alter the photophysical properties. For example, axial coordination of nitrogen ligands to porphyrin metal centers desymmetrizes covalent, cyclic porphyrin arrays.⁵⁰ This desymmetrization decreases excitonic coupling in the antenna system (Fig. 3). Supramolecular binding can therefore partially localize the exciton in a supramolecular antenna, leading to increased fluorescence of an acceptor upon selective excitation of the donors. Desymmetrization is crucial for the purpose of energy funneling and CS as these are inherently asymmetric processes.⁵¹ Supramolecular interactions aid in this regard and supramolecular donor–acceptor complexes yield superior CS lifetimes compared to covalent analogues.⁵²

When heavy atoms are used in the self-assembly of supramolecular antennae they can quench excited states and indeed decreased fluorescence intensity was first reported by Drain and Lehn.⁵³ This phenomenon can be attributed to singlet to triplet intersystem crossing due to the heavy-atom effect.⁵⁴ Elliott *et al.*



Fig. 3 As the porphyrin dimer becomes excited, energy transfer occurs to the ring with the same rate (~ 1.3 ps) no matter its size ($N = 6, 8, 10, 12$ or 30). A representation of the line-dipole model on the right shows the effect of strain induced by coordination. The transferred excitation is delocalized over 6 porphyrins. Adapted with permission from ref. 50.

attempted to resolve this problem by electronically decoupling (using insulating triazole linkers) both singlet and triplet forming chromophores to heavy-atom coordinating pyridines.⁵⁵ Since all photochemistry is determined by kinetics, metal–ligand based supramolecular assemblies can still be used, for example as the rate for singlet energy transfer competes with the rate for intersystem crossing.⁵⁶ Thus metal–ligand interactions are an interesting strategy to produce chromophore assemblies, but care has to be taken that heavy-atoms can induce triplet formation at the expense of energy efficiency.

Hydrogen bonds are regularly employed for the supramolecular organization of chromophores. Triplet energy transfer,⁵⁷ singlet energy transfer⁵⁸ and electron transfer⁵⁹ are all facilitated by hydrogen-bonding interactions, leading to increased rates of transfer due to D–A orbital overlap (following the Dexter mechanism of energy transfer or *via* PET).

Clearly, supramolecular bonding interactions are not innocent and their use complicates the study of light-harvesting assemblies. However, careful use of self-assembly by supramolecular interactions can provide directionality of energy and electron transfer and can lead to increased CS state lifetime as well. Therefore, they are useful in the development of artificial photosynthesis. The influence of supramolecular bonds on photophysics is well explored. Now is the time to use these bonds for the integration of the fundamental actions of photosynthesis. Below examples will illustrate that otherwise inaccessible structures are obtained using self-assembly strategies, that above all show enhanced light-harvesting functionality over covalent analogues.

3.3 Selected examples of supramolecular strategies to construct light harvesting and charge separation systems

The group of Kuroda attempted to generate large size antenna systems using non-covalent strategies.⁶⁰ Hydrogen-bonding interactions have been used in conjunction with metal-porphyrin coordination, all based on multiple interactions to reach high binding constants such that these dyads are formed efficiently under dilute conditions. A free-base porphyrin was symmetrically substituted with spacers at the 4'-phenyl



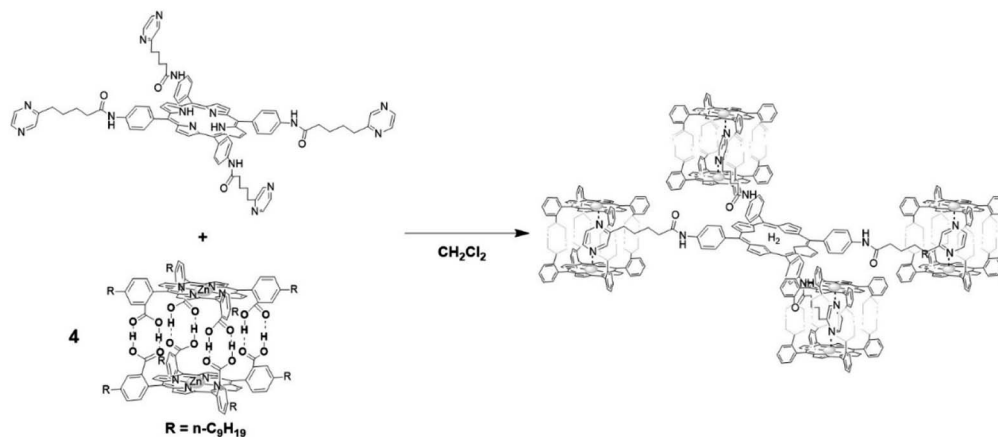


Fig. 4 A porphyrin acceptor functionalized with ditopic pyrazine units (top) that act as guests to the donor Zn-porphyrin cage assembled with hydrogen bonds. A 8 : 1 donor : acceptor ratio is achieved here. Some atoms in the antenna system are omitted for clarity.

positions linked to pyrazine units. These ditopic nitrogen ligands act as a guest by coordinating Zn-porphyrin cages that in turn are formed *via* multiple hydrogen bonds. As such, a single H₂-porphyrin binds 8 light-harvesting Zn-porphyrins (Fig. 4). The energy transfer efficiency from a single Zn-porphyrin cage to the free base was found to be 82%, somewhat lower than previously reported related covalent systems. However, the fluorescence of the free base in the self-assembled structure is enhanced 18-fold demonstrating the antenna effect. More elaborate H₂-porphyrins with increasing pyrazine functionalities linked in a linear or branching topology revealed that the enhanced light-absorption could be further increased (77-fold) when the ratio of 16 : 1 for Zn : H₂ porphyrin was reached.⁶¹

Dendrimers are hyperbranched well-defined macromolecular structures that are prepared in iterative stepwise synthetic

procedures. These structures are interesting scaffolds for applications as light-harvesting antennae, for example by the functionalization of the end groups with porphyrin dyes. Even more interesting is that simple addition of a coordinating C₆₀ acceptor, turns a porphyrin dendrimer into an integrated light-harvesting assembly (Fig. 5).⁶² The authors observed excited-state energy migration across the porphyrins, as is also typically observed in the natural LH system, and an impressively long charge-separated lifetime after PET to the C₆₀ (0.25 ms).

In a supramolecular tour-de-force Kobuke's group developed an integrated light harvesting system that could be extended to CS assembly.^{63,64} The supramolecular antenna was formed by using imidazolyl substituted Zn(II)-porphyrin building blocks. The nonameric porphyrin antenna possessed three Zn-porphyrins that did not partake in the assembly. Thus, simply mixing in a pyridinyl tripodal ligand containing an energy accepting porphyrin and covalently attached fullerene electron acceptor provided an integrated assembly (Fig. 6). The supramolecular structure attained a total energy conversion efficiency of 85% where the charge-separated state had a half-life of 0.2 μs. The authors took their approach even further when they incorporated supramolecular antennae into lipid bilayers (known as dynamic self-assembled interfaces, *vide infra*).⁶⁵



Fig. 5 Dendrimer with 16 porphyrin units act as a light-harvesting antenna, and achieves long lasting charge separation when electron accepting fullerenes bind the porphyrin metal atom. Used with permission from ref. 62.

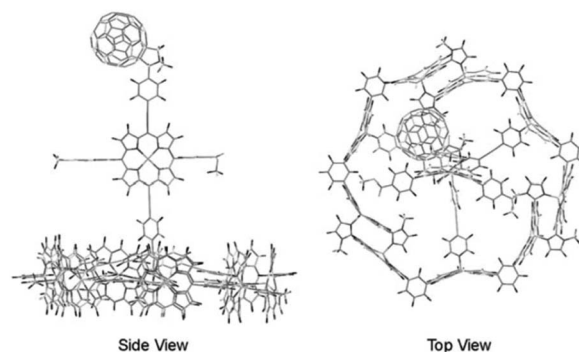


Fig. 6 Atomistic model of an integrated antenna/charge-separation assembly. Adapted with permission from ref. 64.



Transient experiments were not performed, but the authors deduced inter antenna energy transfer between the different antenna systems assembled within the membrane.

Above examples have illustrated that light harvesting architectures can be built using supramolecular strategies that collect photons and transfer their energy over considerable distances. Though supramolecular interactions add to overall complexity of the system, they are a vital tool for assembling multi-chromophoric antennae and integrating them with charge-separation functionality. Such well-organized multi-chromophoric systems often yield enhanced properties such as increased absorption, panchromaticity and charge-separation lifetimes (*i.e.* lowered recombination rates) vital to efficient artificial photosynthesis devices. Meanwhile, these complex structures can be constructed from simple components with high-absorption coefficients that assemble with little synthetic effort and when properly designed, conserve energy and prevent degradative processes by circumventing triplet formation. The ability to direct energy through a supramolecular assembly may prove crucial to collect, transfer and funnel energy for the purpose of artificial photosynthesis. Proper connection to redox catalysis is yet to be demonstrated, however, the implementation of integrated supramolecular antennae/CS assemblies in an artificial photosynthetic device warrants reduced recombination and increased overall photon efficiency. Indeed, when supramolecular interactions are used to preorganize dyes for light-harvesting and CS onto conducting solid materials enhanced device performance is often reported (see Section 6.1).

4 Supramolecular catalysis

For the efficient conversion of solar energy into fuel, redox catalysis is essential. In artificial photosynthetic devices water oxidation provides electrons and protons, whereas proton reduction (or CO₂ reduction) delivers the fuel in an overall thermodynamically uphill reaction. The rate of these multi-electron processes is limited by the photon flux, which provides the redox equivalents with a certain speed. This means that reactive intermediates are produced that should be sufficiently stable to prevent decomposition or recombination. The redox catalysis is mostly performed by transition metals since they can access several oxidation states. Important properties for the catalysts used in artificial photosynthetic devices are (1) catalysis at low overpotential as overpotential leads to losses (2) stability of the catalyst (3) the rate of the catalyst such that the amount of catalyst can be optimized. Supramolecular strategies provide handles to optimize catalysts with respect to these properties. This section focusses on catalysis for artificial photosynthesis using the supramolecular approach. Whereas eventually these properties should be evaluated in a light driven device, these basic properties are easily measured using electrocatalysis or catalysis driven by chemical oxidants/reductants.

4.1 Chemical and electrochemical water oxidation

A key reaction in natural photosynthesis is the oxidation of water, which is benign and abundant, providing electrons and

protons for the production of the fuel. Water oxidation catalysis provides four protons and four electrons from two water molecules leading to the formation of dioxygen. Interestingly, PSII operates using a CaMn₄O₅-cluster. Therefore, chemists have developed analogous clusters that mimic the activity of PSII, but these show low stability and activity at least partly because these synthetic clusters lack the protein environment.⁶⁶ The best synthetic catalyst for water oxidation are currently based on ruthenium and iridium, and in this section we will describe how supramolecular strategies can be used to further increase the performance of these catalysts. The power of supramolecular strategies is illustrated by simple water oxidation catalyst (WOC) that operate *via* a dinuclear mechanism, facilitated by π - π stacking interactions,^{67,68} as well as more complex multi-component systems. To explain this supramolecular effect rationally, the catalytic cycle for water oxidation is explained first.

4.1.1 Mechanisms and potential of supramolecular water oxidation catalysis. WOC can generally operate *via* the mononuclear water nucleophilic attack (WNA) mechanism or the dinuclear radical oxo-coupling (ROC) also known as interaction of two M-O units (I2M) mechanism (Fig. 7). Interestingly, the catalytic mechanism followed has consequences for the properties of the system such as the overpotential that is required and the optimal concentration window of the catalyst. The dinuclear ROC mechanism is favored in terms of overpotential as less intermediates are formed putting less restrictions for optimization as dictated by scaling relationships.⁶⁹ More specifically, it avoids the high energy M-O-O-H intermediate that is formed during the WNA mechanism. Catalysts that follow the ROC mechanism, require two metallo-oxo species to react, which in principle is facilitated by higher concentrations. Dinuclear complexes could in principle achieve this in an intramolecular fashion, however, the M-O-O-M intermediate has a very different optimal M-M distance than two M-OH intermediates.⁶⁷ Therefore, ligand frameworks incorporating



Fig. 7 Water oxidation catalysis follows either of two mechanisms. A mononuclear WNA mechanism or the binuclear ROC mechanism. Used with permission from ref. 69.



Perspective

two metal sites, with a fixed M–M distance, often do not result in great activity.

Catalysts that operate *via* the ROC mechanism could also be preorganized using supramolecular strategies, because supramolecular chemistry can aid in the spatial organization of two metallo-oxo species without exerting a fixed M–M distance.

4.1.2 Selected examples of supramolecular water oxidation. In 2009 the group of Sun reported a Ru-WOC with a 2,2'-bipyridine-6,6'-dicarboxylic acid (bda) ligand and two axial ligands, which follows the dinuclear ROC mechanism.⁷⁰ In 2012 they realized that π - π interactions can assist in bringing two catalysts together in a favorable orientation. Complexes with isoquinoline ligands instead of pyridine enhanced rates greatly, leading to a turn over frequency (TOF) of $>300\text{ s}^{-1}$ and a turn over number (TON) above 8000.⁷¹ Richmond *et al.* also exploited the π - π stacking of the Ru(bda) type catalysts, showing that methoxy substituted isoquinolines enhance π - π stacking increasing the rate (TOF > 900).⁶⁸ Interestingly, they also report a negative example. Axial ligands with cationic functional groups cause repulsion of two complexes. This led to an order of magnitude slower catalysis. The group of Concepcion reported on systematic variations of the axial ligand to enhance the π - π interaction that brings these complexes together in the oxygen bond forming step, which resulted in complexes that display even higher TOFs and TONs of up to 1270 s^{-1} and 27 000 respectively.⁷²

Besides π - π stacking to bring catalysts together, concentrating catalysts by putting them in a confined space is beneficial. In 2012 the groups of Yang and Li showed that confining Ru(bda)(pic)₂ (pic = picoline) WOCs in mesoporous silica led to improved TOFs (Fig. 8).⁷³ Interestingly, the use of different sizes of amphiphilic RuWOCs can lead to selection between the mononuclear WNA mechanism and the dinuclear ROC mechanism (Fig. 9).⁷⁴ Yang *et al.* showed that the use of amphiphilic groups on the axial ligands of Ru(bda) systems led to self-assembly of liposome-like structures. A large amphiphilic substituent increased the Ru–Ru distance which inhibited the ROC mechanism, but a small amphiphilic group favored the ROC mechanism resulting in faster catalysis.

Supramolecular interactions are also exploited to increase local concentrations facilitating electrochemical water oxidation, as showcased by our group in 2018.⁷⁵ We incorporated increasing equivalents of sulfonated Ru-WOC in a guanidinium functionalized M₁₂L₂₄ supramolecular cage (Fig. 10). Interestingly, the rate of catalysts that follow the dinuclear ROC mechanism was enhanced up to 130 times through encapsulation, while the rate of a Ru-WOC that operates *via* the mononuclear WNA mechanism was unchanged by increasing

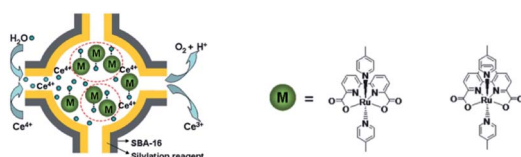


Fig. 8 WOC encapsulated in mesoporous silica. Used with permission from ref. 73.



Fig. 9 Alkyl chain substituted WOC self-assemble into micellar vesicles in water, preorganizing the WOC for the ROC mechanism. Used with permission from ref. 74.

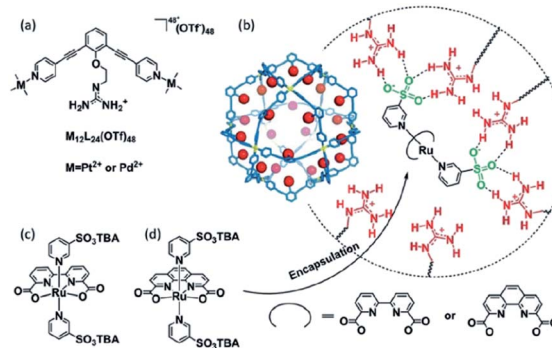


Fig. 10 Sulfonated WOC entrapped in a M₁₂L₂₄ supramolecular sphere. Used with permission from ref. 75.

the local concentration. This example shows that great rate enhancements can be achieved by spatial organization of catalytically active species following the dinuclear mechanism.

The group of Würthner showed that ditopic pyridinyl ligands bind the axial positions of Ru(bda) complexes resulting in the formation of a supramolecular macrocycle catalyst trimer, [Ru(bda)bpb]₃.⁷⁶ They showed that supramolecular interactions spread out the catalytic sites while capable of oxidizing water using the WNA mechanism. These trimers showed exceptionally stable, due to limited accessibility of the active sites by steric repulsion of the organic scaffolds. A follow-up study investigated the effect of the ring size and the role of the hydrogen bonding network between water molecules that reside within the trimeric structure (Fig. 11).⁷⁷ Higher rates were obtained when all reactive sites point towards the interior of the macrocycle, because the favorable hydrogen bonding network stabilizes the generated protons.

4.2 Chemical and electrochemical proton reduction

Water oxidation catalysis provides the electrons and protons that are needed to generate the fuel by a reduction reaction. The



catalyst loadings comparable to metal oxide sensitization were reported, denoting the potential of supramolecular functionalization of electrodes. Besides enhanced stability, polymers facilitating a second coordination may influence reaction selectivity. This was demonstrated by Liu and McCrory, who embedded Co-phtalocyanine CO₂ reduction catalysts in polyvinylpyridines.⁹⁵ They postulated that high CO product selectivity is obtained by sluggish proton transfer through the polymer, while protonated pyridine was sufficiently acidic to act as proton donor to CO₂.

In the above examples the catalytic reactions were evaluated by electrochemical methods, providing insight in the important properties of the catalysts and highlighting the effects of supramolecular encapsulation. Electrochemical methods can also be implemented in artificial photosynthesis using PV-electrolysis set-ups. For the preparation of integrated systems in which light is directly used to generate fuel, supramolecular approaches can also be fruitful and this will be discussed in the next section.

5 Supramolecular artificial photosynthesis

Supramolecular assemblies are mainly explored for light-driven water oxidation, proton reduction and to a lesser extent for CO₂ reduction. The catalytic systems can be divided in two categories. (i) Dye-catalyst assemblies where a light absorbing functionality is preorganized to a molecular catalyst using non-covalent bonds, and (ii) dynamic self-assembled interfaces where dye and catalyst are co-embedded in a self-assembled membrane. These strategies are discussed below.

5.1 Supramolecular photochemical water oxidation

5.1.1 Supramolecular dye-WOC assemblies. In 2012 & 2014 the group of Sun reported Ru(bda) complexes functionalized on the axial ligand with ruthenium complexes that act as chromophore. The self-assembled construct resulted in a four times higher TON in light driven water oxidation than a molecular system based on the free components (38 vs. 8).⁹⁶ In a subsequent approach, a cyclodextrin-modified Ru(bpy)₃ (bpy = 2,2'-



Fig. 17 Supramolecular dye-WOC assemblies are formed by cyclodextrin host-guest chemistry. This results in enhanced stability in photocatalytic water oxidation in presence of a sacrificial oxidant. Cl⁻ ions are omitted.

bipyridine) chromophore was combined with a Ru(bda)(ppy)₂ (ppy = 4-phenylpyridine) catalyst in which the preorganization of the chromophore and catalyst was achieved by binding of the hydrophobic axial ligand into the cage of the CD (Fig. 17).⁹⁷ Again a higher TON (267) in light driven water oxidation was reported for the supramolecular construct compared to the control experiments. When either the CD functionality was omitted or the ppy ligand was replaced for a pic ligand, which is not significantly bound in the CD, the TON dropped by an order of magnitude. It is important to note that in these examples the TON increases, showing that the preorganization has an impact on the stability of the system. The effect of such preorganization on the solar to fuel efficiency has yet to be reported.

Cobalt based polyoxometalates (POMs) are water oxidation catalysts and were preorganized to light absorbing carbon nanodots using electrostatic interactions.⁹⁸ The supramolecular construct was used in light driven water oxidation, resulting in TONs up to 552. Paille and co-workers investigated metal organic frameworks (MOF), such as MOF-545 as a light-absorbing supramolecular host for water oxidation catalysts.⁹⁹ They chose a POM [(PW₉O₃₄)₂Co₄(H₂O)₂]¹⁰⁻ as the WOC, which was immobilized in the MOF by mild aqueous impregnation (Fig. 18). This system reached a TON of 70 per POM after one hour of photocatalysis and could be recovered after catalysis by filtration, retaining most of its activity. The authors mentioned that the sacrificial oxidant was limiting the conversion. All control experiments in which one of the components was absent, showed low conversion, denoting the importance of both the catalyst-sensitizer preorganization and enhanced POM stability when encapsulated. When the supramolecular assembly is loaded on thin films, the TON is increased 23-fold.¹⁰⁰

Bonchio *et al.* wanted to increase the dye-catalyst ratio, as this is also found in natural photosynthesis. By using a Ru-POM structure as water oxidation catalyst, a dye-WOC assembly was formed in 5 : 1 ratio.¹⁰¹ The catalyst intercalated into π -stacked



Fig. 18 The components (left) are the catalytic POM (top) light-harvesting porphyrin strut (middle) and structural Zr-cluster (bottom) that lead to a supramolecular artificial photosynthetic assembly (right). Used with permission from ref. 99.



that in the natural system light energy is converted into chemical fuel both by the proton gradient across the membrane, as well as light driven proton reduction to form protonated nicotinamide adenine dinucleotide (NADH), and that this system is one rare mimic of the former.

A similar system was reported in the group of Matile.¹²¹ Self-assembled naphthalene diimide (NDI) rigid-rods breached unilamellar vesicles to allow photosynthetic energy conversion. EDTA was oxidized at the exterior, while internal quinones could be reduced at the interior of the vesicle.

Besides vesicles other soft materials can be considered as exemplified by the supramolecular hydrogel scaffolds reported Wasielewski and Stupp.¹²² Perylene monoimide amphiphiles acted as chromophores and self-assembled into a 3D scaffold, that preorganized HEC using electrostatic interactions.

6 Supramolecular photosynthetic devices

The state-of-the-art applications for artificial photosynthesis focused on DSSC and DS-PEC devices, as discussed in Section 2, suffer from recombination processes lowering the efficiency. Moreover, the catalytic processes need optimization as they should require minimal overpotential, are very active and have sufficient stability. The supramolecular strategies discussed in Sections 3–5 address some of these issues, but mostly describe systems that are in homogeneous solutions and are aimed at understanding the role of supramolecular organization on (photo)chemical and (photo)catalytic properties of assemblies. In the next section, we will focus on a few studies that have actually employed supramolecular strategies in functional devices.

6.1 Supramolecular DSSC

6.1.1 n-type. In current DSSC the electron transfer between the redox mediator and the dye is of pure collisional nature. Supramolecular chemistry provides a tool to preorganize the mediator to the dye to promote efficient electron propagation through the system. Berlinguette and co-workers have shown that dye regeneration can be optimized by halogen bonding leading to a higher V_{OC} and PCE (Fig. 30).¹²³ Furthermore,



Fig. 30 The redox mediator binds the dye after electron injection due to halogen-bonding substituents on the dye. It is then quickly regenerated and as a result back electron transfer is inhibited. Used with permission from ref. 123.

preorganization of Li^+ ions close to the dye increases the local concentration of I^- , and results in decreased recombination.¹²⁴

Supramolecular antennae as discussed in Section 3 are applied in n-type DSSC. J-aggregates have been assembled by spin-coating Zn-porphyrin solutions onto TiO_2 .¹²⁵ Interestingly, free base porphyrins heterogenized on TiO_2 could be self-assembled with spherical agglomerates of Zn-porphyrins *via* H-bonding diphenylalanine substitutions (Fig. 31).¹²⁶ The implementation of such antenna led to a doubling of the DSSC efficiency showing that implementation of supramolecular antennae can considerably boost the efficiency in devices.

Additional strategies reported in this area are a TiO_2 functionalized material with coordinating ligands that bind porphyrins in multi-chromophoric assemblies.¹²⁷ It also has been demonstrated that supramolecular porphyrin assemblies on TiO_2 inhibit charge-recombination by stepwise charge separation.¹²⁸

6.1.2 p-type. The p-type DSSC's in general suffer from high recombination rates, leading to low efficiencies. This needs to be considerably improved for application or for the construction of tandem DS-PEC devices. Whereas most work has been devoted to dye optimization, *i.e.* the generation of polar chromophores, we have explored the use of supramolecular approaches to suppress charge recombination. Pseudorotaxanes are used in p-type DSSC to preorganize the dye and the redox mediator (Fig. 32). The binding constant of a charge-carrying ring that acts as the redox mediator is lower upon photoelectrochemical reduction, improving charge-separation.¹²⁹ In the first prototype device the famous “blue box” developed by Stoddart is used as ring and redox mediator. The dye is functionalized with a naphthalene functional group as thread (P_N), and it is known that upon reduction of the blue box, the ring loses its affinity for this particular recognition site, allowing it to dethread to be replaced by another ring. The study revealed a 10-fold increase in photocurrent in presence of the ring and the dye with the thread as recognition site, compared to the control experiments in which this interaction is not



Fig. 31 Supramolecular antenna complexes are assembled onto n-type semi-conductors (TiO_2) using hydrogen-bonding interactions. H_2 -porphyrin acceptor (blue discs) act as the seed for the growth of Zn-porphyrin antennae acting as energy donor. Used with permission from ref. 126.



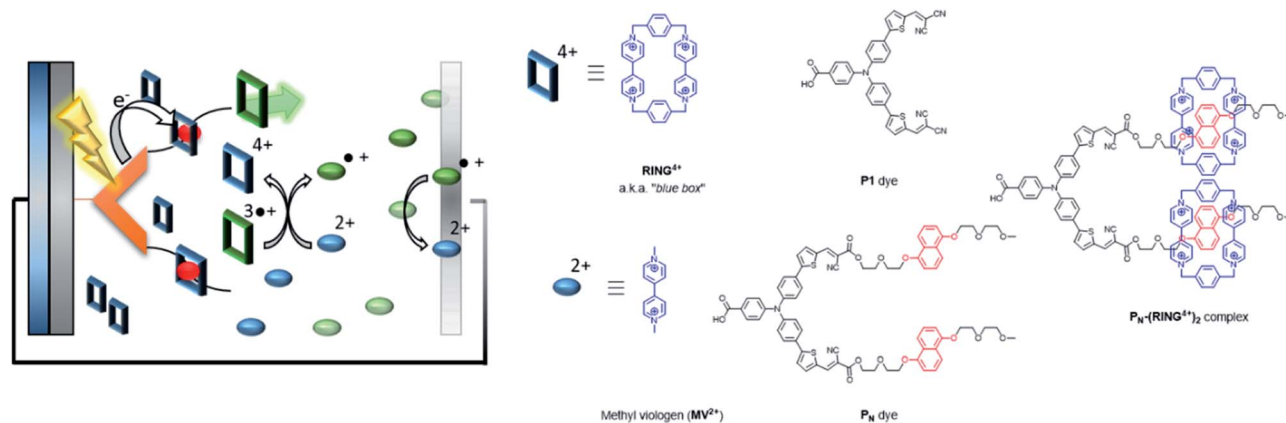


Fig. 32 Supramolecular interactions are implemented in p-type DSSC using the "blue box" as redox shuttle. The P_N dye is heterogenized onto NiO, and binds the ring prior to excitation. As soon as the ring is reduced, it loses affinity for the chromophore, dethreads and moves away while carrying the charge. Used with permission from ref. 129.

present. The explanation for the increase in efficiency is twofold. Firstly, dye–mediator interactions preorganize the mediator to readily accept an electron from the photo-reduced dye, preventing charge recombination with the semiconductor. Secondly, the low local concentration of reduced ring by this displacement also leads to lower charge recombination.

6.1.3 Supramolecular p/n junctions. Silicon solar cells have a so-called p/n-junction, a layer of n-doped on top of p-doped silicon. This p/n-junction provides a driving force for CS, allowing excited electrons to flow from the anode (p-type) side to the cathode side (n-type) of the device. A molecular analogue of such a system consists of an electron donor (D) light-absorber (C) and electron acceptor (A).

Implementation of supramolecular Zr^{IV} -phosphonate chemistry developed in the group of Mallouk provides a tool to create layer-by-layer assemblies.¹³⁰ By sequentially dipping a metal-oxide (ITO, TiO_2 , NiO) coated glass slide in solution of phosphonic acid functionalized components alternated by a Zr^{IV} solution, Meyer and co-workers synthesized an assembly purely based on molecular components with long lived

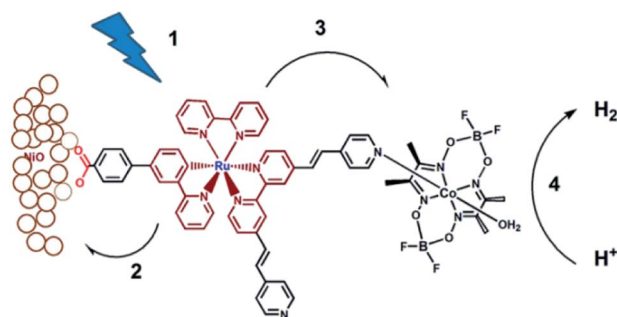


Fig. 34 The dye-HEC assembly is anchored to NiO to produce a functional DS-PEC producing molecular hydrogen under illumination. The catalyst is preorganized to the dye by a dative, stable during operation. Used with permission from ref. 134.

photoinduced charge separated states that function as p/n-junctions (Fig. 33).¹³¹ Electron recombination occurred after 5.6 s for the photoanode and an impressive 26 ms for the photocathode. This bottom-up approach is very promising for future hybrid technologies, and has already been implemented in the preparation of supramolecular DS-PEC (*vide infra*).

Supramolecular p/n junctions can also be obtained *via* π - π stacking, NDI's based, zippers. By electronically tuning the

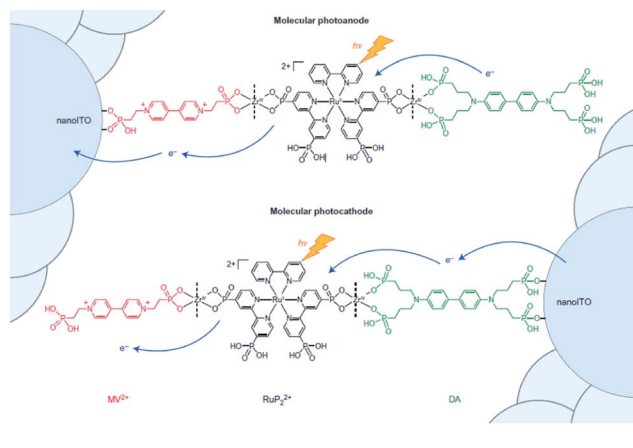


Fig. 33 Molecular p/n-junctions are accessible by supramolecular Zr^{IV} -phosphonate chemistry. Used with permission from ref. 131.

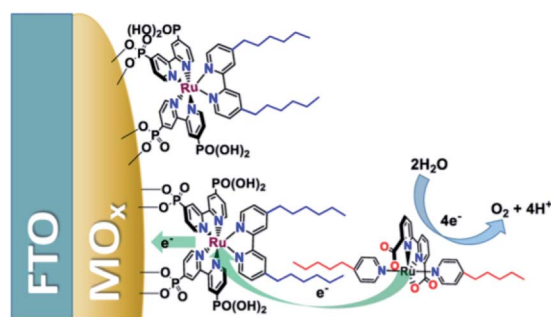


Fig. 35 Heterogenized dyes bear aliphatic tails, allowing for supramolecular preorganization of Ru-WOC in DS-PEC devices. Used with permission from ref. 137.



catalyst properties. For water oxidation catalysis, two reaction pathways are known, and the one that proceeds *via* a dinuclear mechanism can be stimulated and enhanced by supramolecular preorganization. In addition, supramolecular preorganization of the catalyst and the substrate, leading to high local concentrations, also enhances catalysis as is demonstrated for proton reduction catalysis. Catalyst stability is one of the key parameters to optimize, and encapsulation of catalysts in supramolecular cages can prevent degradation of catalysts, for example by preventing (dinuclear) disproportionation of reactive intermediates. Supramolecular preorganization can also be used to construct devices and electrodes, and preorganization of redox mediators and chromophores in DSSC have resulted in higher efficiencies.

So far mostly components for artificial photosynthetic devices have been explored. The next challenge is to implement the components responsible for the different actions of artificial photosynthesis in working devices. Next to using components that use some of the discussed supramolecular strategies, self-assembly could also be to generate the highly organized, complex molecular architectures within the device. Supramolecular chemistry does not only enable facile synthesis of assemblies such as antennae, charge-separating and catalytic components, it may also allow for their integration into a fully artificial photosynthetic device. Such an assembly will be heavily inspired by natural photosynthesis, but may be simplified and more robust. We are looking forward to the days that these assemblies are coupled to inorganic materials, showing high efficiency and stability as operative DS-PEC.

Conflicts of interest

There are no conflicts to declare.

Acknowledgements

This work has been funded by the Netherlands Organisation for Scientific Research (NWO) and National Science Foundation China (NSFC) as part of the program Cooperation China (NSFC) – Supramolecular Chemistry & Catalysis and was supported by the Holland Research School of Molecular Chemistry (HRSMC) and Foundation for Fundamental Research on Matter (FOM), which is part of NWO.

Notes and references

- N. S. Lewis and D. G. Nocera, *Proc. Natl. Acad. Sci. U. S. A.*, 2006, **103**, 15729–15735.
- S. Berardi, S. Drouet, L. Francàs, C. Gimbert-Suriñach, M. Guttentag, C. Richmond, T. Stoll and A. Llobet, *Chem. Soc. Rev.*, 2014, **43**, 7501–7519.
- M. Roeb and H. Müller-Steinhagen, *Science*, 2010, **329**, 773–774.
- N. Armaroli and V. Balzani, *Chem.–Eur. J.*, 2016, **22**, 32–57.
- R. J. Detz, K. Sakai, L. Spiccia, G. W. Brudvig, L. Sun and J. N. H. Reek, *ChemPlusChem*, 2016, **81**, 1024–1027.
- M. D. Kärkäs, O. Verho, E. V. Johnston and B. Åkermark, *Chem. Rev.*, 2014, **114**, 11863–12001.
- D. Gust, T. A. Moore and A. L. Moore, *Acc. Chem. Res.*, 2009, **42**, 1890–1898.
- V. Balzani, A. Credi and M. Venturi, *Curr. Opin. Chem. Biol.*, 1997, **1**, 506–513.
- R. Croce and H. Van Amerongen, *Nat. Chem. Biol.*, 2014, **10**, 492–501.
- P. Knörzer, A. Silakov, C. E. Foster, F. A. Armstrong, W. Lubitz and T. Happe, *J. Biol. Chem.*, 2012, **287**, 1489–1499.
- J. M. Lehn, *Angew. Chem., Int. Ed.*, 2013, **52**, 2836–2850.
- T. J. Jacobsson, V. Fjällström, M. Edoff and T. Edvinsson, *Energy Environ. Sci.*, 2014, **7**, 2056–2070.
- A. V. Akimov, A. J. Neukirch and O. V. Prezhdo, *Chem. Rev.*, 2013, **113**, 4496–4565.
- F. Li, K. Fan, B. Xu, E. Gabrielsson, Q. Daniel, L. Li and L. Sun, *J. Am. Chem. Soc.*, 2015, **137**, 9153–9159.
- G. Peharz, F. Dimroth and U. Wittstadt, *Int. J. Hydrogen Energy*, 2007, **32**, 3248–3252.
- J. Jia, L. C. Seitz, J. D. Benck, Y. Huo, Y. Chen, J. W. D. Ng, T. Bilir, J. S. Harris and T. F. Jaramillo, *Nat. Commun.*, 2016, **7**, 13237.
- A. Fujishima and K. Honda, *Nature*, 1972, **238**, 37–38.
- T. Hisatomi and K. Domen, *Nat. Catal.*, 2019, **2**, 387–399.
- D. G. Nocera, *Acc. Chem. Res.*, 2012, **45**, 767–776.
- B. O'Regan and M. Grätzel, *Nature*, 1991, **353**, 737–740.
- A. Hagfeldt, G. Boschloo, L. Sun, L. Kloo and H. Pettersson, *Chem. Rev.*, 2010, **110**, 6595–6663.
- M. Pazoki, U. B. Cappel, E. M. J. Johansson, A. Hagfeldt and G. Boschloo, *Energy Environ. Sci.*, 2017, **10**, 672–709.
- E. Benazzi, J. Mallows, G. H. Summers, F. A. Black and E. A. Gibson, *J. Mater. Chem. C*, 2019, **7**, 10409–10445.
- H. J. Snaith, *Nat. Photonics*, 2012, **6**, 337–340.
- X. Yang, M. Yanagida and L. Han, *Energy Environ. Sci.*, 2013, **6**, 54–66.
- J. Halme, P. Vahermaa, K. Miettunen and P. Lund, *Adv. Mater.*, 2010, **22**, E210–E234.
- K. Takagi, S. Magaino, H. Saito, T. Aoki and D. Aoki, *J. Photochem. Photobiol., C*, 2013, **14**, 1–12.
- P. R. F. Barnes, K. Miettunen, X. Li, A. Y. Anderson, M. Bessho, T. Grazel and B. C. O'Regan, *Adv. Mater.*, 2013, **25**, 1881–1922.
- R. Katoh and A. Furube, *J. Photochem. Photobiol., C*, 2014, **20**, 1–16.
- F. Fabregat-Santiago, G. Garcia-Belmonte, I. Mora-Sero and J. Bisquert, *Phys. Chem. Chem. Phys.*, 2011, **13**, 9083–9118.
- E. M. J. Johansson, R. Lindblad, H. Siegbahn and A. Hagfeldt, *ChemPhysChem*, 2014, **15**, 1006–1017.
- H. N. Tsao, C. Yi, T. Moehl, J. H. Yum, S. M. Zakeeruddin, M. K. Nazeeruddin and M. Grätzel, *ChemSusChem*, 2011, **4**, 591–594.
- S. Mathew, A. Yella, P. Gao, R. Humphry-Baker, B. F. E. Curchod, N. Ashari-Astani, I. Tavernelli, U. Rothlisberger, M. K. Nazeeruddin and M. Grätzel, *Nat. Chem.*, 2014, **6**, 242–247.



- M. Rousset and C. Léger, *J. Am. Chem. Soc.*, 2006, **128**, 5209–5218.
- 82 B. Ginovska-Pangovska, A. Dutta, M. L. Reback, J. C. Linehan and W. J. Shaw, *Acc. Chem. Res.*, 2014, **47**, 55.
- 83 A. Pannwitz and O. S. Wenger, *Chem. Commun.*, 2019, **55**, 4004–4014.
- 84 M. L. Helm, M. P. Stewart, R. M. Bullock, M. R. DuBois and D. L. DuBois, *Science*, 2011, **333**, 863–866.
- 85 J. Duan, S. Mebs, K. Laun, F. Wittkamp, J. Heberle, T. Happe, E. Hofmann, U. P. Apfel, M. Winkler, M. Senger, M. Haumann and S. T. Stripp, *ACS Catal.*, 2019, **9**, 9140–9149.
- 86 A. Dutta, A. M. Appel and W. J. Shaw, *Nat. Rev. Chem.*, 2018, **2**, 244–252.
- 87 M. L. Singleton, J. H. Reibenspies and M. Y. Darensbourg, *J. Am. Chem. Soc.*, 2010, **132**, 8870–8871.
- 88 M. L. Singleton, D. J. Crouthers, R. P. Duttweiler, J. H. Reibenspies and M. Y. Darensbourg, *Inorg. Chem.*, 2011, **50**, 5015–5026.
- 89 F. J. Rizzuto, L. K. S. von Krbek and J. R. Nitschke, *Nat. Rev. Chem.*, 2019, **3**, 204–222.
- 90 S. S. Nurttila, R. Zaffaroni, S. Mathew and J. N. H. Reek, *Chem. Commun.*, 2019, **55**, 3081–3084.
- 91 R. Zaffaroni, N. Orth, I. Ivanović-Burmazović and J. N. H. Reek, *Angew. Chem. Int. Ed.*, 2020, **59**, 18485–18489.
- 92 R. Zaffaroni, E. O. Bobylev, R. Plessius, J. I. van der Vlugt and J. N. H. Reek, *J. Am. Chem. Soc.*, 2020, **142**, 8837–8847.
- 93 W. P. Brezinski, M. Karayilan, K. E. Clary, N. G. Pavlopoulos, S. Li, L. Fu, K. Matyjaszewski, D. H. Evans, R. S. Glass, D. L. Lichtenberger and J. Pyun, *Angew. Chem., Int. Ed.*, 2018, **57**, 11898–11902.
- 94 B. Reuillard, J. Warnan, J. J. Leung, D. W. Wakerley and E. Reisner, *Angew. Chem.*, 2016, **128**, 4020–4025.
- 95 Y. Liu and C. C. L. McCrory, *Nat. Commun.*, 2019, **10**, 1–10.
- 96 F. Li, Y. Jiang, B. Zhang, F. Huang, Y. Gao and L. Sun, *Angew. Chem., Int. Ed.*, 2012, **51**, 2417–2420.
- 97 H. Li, F. Li, B. Zhang, X. Zhou, F. Yu and L. Sun, *J. Am. Chem. Soc.*, 2015, **137**, 4332–4335.
- 98 Y. Choi, D. Jeon, Y. Choi, J. Ryu and B. S. Kim, *ACS Appl. Mater. Interfaces*, 2018, **10**, 13434–13441.
- 99 G. Paille, M. Gomez-Mingot, C. Roch-Marchal, B. Lassalle-Kaiser, P. Mialane, M. Fontecave, C. Mellot-Draznieks and A. Dolbecq, *J. Am. Chem. Soc.*, 2018, **140**, 3613–3618.
- 100 G. Paille, M. Gomez-Mingot, C. Roch-Marchal, M. Haouas, Y. Benseghir, T. Pino, M. H. Ha-Thi, G. Landrot, P. Mialane, M. Fontecave, A. Dolbecq and C. Mellot-Draznieks, *ACS Appl. Mater. Interfaces*, 2019, **11**, 47837–47845.
- 101 M. Bonchio, Z. Syrgiannis, M. Burian, N. Marino, E. Pizzolato, K. Dirian, F. Rigodanza, G. A. Volpato, G. La Ganga, N. Demitri, S. Berardi, H. Amenitsch, D. M. Guldi, S. Caramori, C. A. Bignozzi, A. Sartorel and M. Prato, *Nat. Chem.*, 2019, **11**, 146–153.
- 102 X. Jing, Y. Yang, C. He, Z. Chang, J. N. H. Reek and C. Duan, *Angew. Chem., Int. Ed.*, 2017, **56**, 11759–11763.
- 103 A. F. Heyduk and D. G. Nocera, *Science*, 2001, **293**, 1639–1641.
- 104 V. Artero, M. Chavarot-Kerlidou and M. Fontecave, *Angew. Chem., Int. Ed.*, 2011, **50**, 7238–7266.
- 105 A. Fihri, V. Artero, M. Razavet, C. Baffert, W. Leibl and M. Fontecave, *Angew. Chem., Int. Ed.*, 2008, **47**, 564–567.
- 106 C. Li, M. Wang, J. Pan, P. Zhang, R. Zhang and L. Sun, *J. Organomet. Chem.*, 2009, **649**, 2814–2819.
- 107 W. Lubitz, E. J. Reijerse and J. Messinger, *Energy Environ. Sci.*, 2008, **1**, 15–31.
- 108 F. Gloaguen and T. B. Rauchfuss, *Chem. Soc. Rev.*, 2009, **38**, 100–108.
- 109 A. M. Kluwer, R. Kapre, F. Hartl, M. Lutz, A. L. Spek, A. M. Brouwer, P. W. N. M. Van Leeuwen and J. N. H. Reek, *Proc. Natl. Acad. Sci. U. S. A.*, 2009, **106**, 10460–10465.
- 110 S. Pullen, H. Fei, A. Orthaber, S. M. Cohen and S. Ott, *J. Am. Chem. Soc.*, 2013, **135**, 16997–17003.
- 111 K. Sasan, Q. Lin, C. Mao and P. Feng, *Chem. Commun.*, 2014, **50**, 10390–10393.
- 112 X. Jing, C. He, Y. Yang and C. Duan, *J. Am. Chem. Soc.*, 2015, **137**, 3967–3974.
- 113 C. Orain, F. Quentel and F. Gloaguen, *ChemSusChem*, 2014, **7**, 638–643.
- 114 M. Hansen, S. Troppmann and B. König, *Chem.–Eur. J.*, 2016, **22**, 58–72.
- 115 K. Watanabe, K. Moriya, T. Kouyama, A. Onoda, T. Minatani, S. Y. Takizawa and S. Murata, *J. Photochem. Photobiol., A*, 2011, **221**, 113–122.
- 116 L. He, C. Luo, Y. Hou, C. Li, Q. Zhou, Y. Sun, W. Wang, B. Zhang and X. Wang, *Int. J. Hydrogen Energy*, 2011, **36**, 10593–10599.
- 117 H.-Y. Wang, W.-G. Wang, G. Si, F. Wang, C.-H. Tung and L.-Z. Wu, *Langmuir*, 2010, **26**, 9766–9771.
- 118 S. Troppmann and B. König, *Chem.–Eur. J.*, 2014, **20**, 14570–14574.
- 119 R. Becker, T. Bouwens, E. C. F. Schippers, T. Gelderen, M. Hilbers, S. Woutersen and J. N. H. Reek, *Chem.–Eur. J.*, 2019, **25**, 13921–13929.
- 120 G. Steinberg-Yfrach, J. L. Rigaud, E. N. Durantini, A. L. Moore, D. Gust and T. A. Moore, *Nature*, 1998, **392**, 479–482.
- 121 S. Bhosale, A. L. Sisson, P. Talukdar, A. Fürstnberg, N. Banetji, E. Vauthey, G. Bollot, J. Mareda, C. Röger, F. Würthner, N. Sakai and S. Matile, *Science*, 2006, **313**, 84–86.
- 122 A. S. Weingarten, R. V. Kazantsev, L. C. Palmer, M. McClendon, A. R. Koltonow, A. P. S. Samuel, D. J. Kiebal, M. R. Wasielewski and S. I. Stupp, *Nat. Chem.*, 2014, **6**, 964–970.
- 123 F. G. L. Parlane, C. Mustoe, C. W. Kellett, S. J. Simon, W. B. Swords, G. J. Meyer, P. Kennepohl and C. P. Berlinguette, *Nat. Commun.*, 2017, **8**, 1761.
- 124 Y. Uemura, T. N. Murakami and N. Koumura, *J. Phys. Chem. C*, 2014, **118**, 16749–16759.
- 125 A. Huijser, B. M. J. M. Suijkerbuijk, R. J. M. K. Gebbink, T. J. Savenije and L. D. A. Siebbeles, *J. Am. Chem. Soc.*, 2008, **130**, 2485–2492.



- 126 G. Charalambidis, K. Karikis, E. Georgilis, B. L. M'Sabah, Y. Pellegrin, A. Planchat, B. Lucas, A. Mitraki, J. Bouclé, F. Odobel and A. G. Coutsolelos, *Sustainable Energy Fuels*, 2017, **1**, 387–395.
- 127 N. K. Subbaiyan, C. A. Wijesinghe and F. D'Souza, *J. Am. Chem. Soc.*, 2009, **131**, 14646–14647.
- 128 M. Planells, L. Pellejà, P. Ballester and E. Palomares, *Energy Environ. Sci.*, 2011, **4**, 528–534.
- 129 T. Bouwens, S. Mathew and J. N. H. Reek, *Faraday Discuss.*, 2019, **215**, 393–406.
- 130 G. Cao, H. G. Hong and T. E. Mallouk, *Acc. Chem. Res.*, 1992, **25**, 420–427.
- 131 B. H. Farnum, K.-R. Wee and T. J. Meyer, *Nat. Chem.*, 2016, **8**, 845–852.
- 132 R. S. K. Kishore, O. Kel, N. Banerji, D. Emery, G. Bollot, J. Mareda, A. Gomez-Casado, P. Jonkheijm, J. Huskens, P. Maroni, M. Borkovec, E. Vauthey, N. Sakai and S. Matile, *J. Am. Chem. Soc.*, 2009, **131**, 11106–11116.
- 133 R. Bhosale, J. Míšek, N. Sakai and S. Matile, *Chem. Soc. Rev.*, 2010, **39**, 138–149.
- 134 Z. Ji, M. He, Z. Huang, U. Ozkan and Y. Wu, *J. Am. Chem. Soc.*, 2013, **135**, 11696–11699.
- 135 X. Ding, Y. Gao, L. Ye, L. Zhang and L. Sun, *ChemSusChem*, 2015, **8**, 3992–3995.
- 136 L. Wang, D. E. Polyansky and J. J. Concepcion, *J. Am. Chem. Soc.*, 2019, **141**, 8020–8024.
- 137 D. Wang, L. Wang, M. D. Brady, C. J. Dares, G. J. Meyer, T. J. Meyer and J. J. Concepcion, *J. Phys. Chem. C*, 2019, **123**, 30039–30045.
- 138 K. Hanson, D. A. Torelli, A. K. Vannucci, M. K. Brennaman, H. Luo, L. Alibabaei, W. Song, D. L. Ashford, M. R. Norris, C. R. K. Glasson, J. J. Concepcion and T. J. Meyer, *Angew. Chem., Int. Ed.*, 2012, **51**, 12782–12785.
- 139 X. Ding, Y. Gao, L. Zhang, Z. Yu, J. Liu and L. Sun, *ACS Catal.*, 2014, **4**, 2347–2350.
- 140 M. A. Gross, C. E. Creissen, K. L. Orchard and E. Reisner, *Chem. Sci.*, 2016, **7**, 5537–5546.
- 141 D. Wang, R. N. Sampaio, L. Troian-Gautier, S. L. Marquard, B. H. Farnum, B. D. Sherman, M. V. Sheridan, C. J. Dares, G. J. Meyer and T. J. Meyer, *J. Am. Chem. Soc.*, 2019, **141**, 7926–7933.
- 142 D. Wang, Y. Wang, M. D. Brady, M. V. Sheridan, B. D. Sherman, B. H. Farnum, Y. Liu, S. L. Marquard, G. J. Meyer, C. J. Dares and T. J. Meyer, *Chem. Sci.*, 2019, **10**, 4436–4444.

